Active optics handling inside Galileo Telescope

F. Bortoletto, D. Fantinel, R. Ragazzoni, C. Bonoli, M. D'Alessandro

Osservatorio Astronomico di Padova
vicolo dell'Osservatorio 5, I–35122-Italy

A. Balestra, P. Marcucci, M. Pucillo, C. Vuerli

Osservatorio Astronomico di Trieste
via Tiepolo 11, I–34131-Italy

ABSTRACT

A large part of the active optics system and control environment for the Galileo telescope has been developed and tested. Presently the primary mirror support cell has been characterized for the mechanical and optical aspects. The primary mirror has also been characterized and tested with the active support system in work.

Part of the mechanics for the secondary and tertiary active mirror supports has been constructed and we plan to start the characterization work in the second half of this year.

An overview of the main results obtained during factory acceptance tests and a discussion about the general informatics implementation is here provided.

1. INTRODUCTION

The Galileo telescope belongs to a new category of telescopes aimed to provide the best performance possible in every observing condition. Like its predecessor, the ESO's New Technology Telescope, the main features at the base of this capability are the innovative building, an accurate tracking system, a broad use of processors dedicated to specific control tasks, and the presence of an active optics system with an extended range of options.

Particular care has been taken to optimize the active optics system, with the aim to monitor and control it also during the real scientific observations. This optimization is based on several modifications, here described, spanning from mechanics and optics to the computer control systems.

2. THE GALILEO PRIMARY MIRROR SYSTEM

The TNG primary mirror cell system is described in detail in Ref.1, here the main properties of the system are reviewed.

Taking into account only the axial support of the mirror (the lateral support system is purely *passive*) we have:

- 75 astatic actuators placed in four rings;
- 3 rigid actuators, placed at 120^0 on the 3^{rd} ring.

Each astatic actuator can be computer driven in order to react at the mirror contact point with a force between 50 and 100 Kg (note that the force range can also be extended, if necessary, making use of springs); this force can be monitored with a precision of about 100 gr through a load-cell. The force delivered by the astatic actuator must take care of the distributed weight of the mirror (*passive force, PF*), the delivery of the force required for mirror elastic deformation (*active force, AF* with nearly zero mean on the overall mirror) and the compensation of force changes when the elevation angle (*EL*) changes.

So the basic behaviour of each astatic support can be described by the *total delivered force, TF*, which is:

$$TF = PF\sin(EL) + AF \tag{1}$$

with the conditions:

0-8194-1494-8/94/$6.00

Mode	$\lambda = 500nm$ @ $EL = 5.7$deg	$\lambda = 500nm$ @ $EL = 23.6$deg
SPH3	1.14λ	4.56λ
AST3	$\pm 3.31\lambda$	$\pm 13.24\lambda$
3COM	$\pm 0.99\lambda$	$\pm 3.96\lambda$
4AST	$\pm 0.43\lambda$	$\pm 1.72\lambda$
COM5	$\pm 0.30\lambda$	$\pm 1.20\lambda$

Table 1: Modal correction dynamics in M1.

$$\sum_{i=1}^{78} PF = MW \quad @EL = 90\text{deg}; \quad \sum_{i=1}^{75} AF = 0 \tag{2}$$

where MW is the total mirror weight. The active term AF must, of course, be kept constant during an elevation slew although, being the actuator based on mechanical levers, the position change will magnify, or demagnify, a given AF pattern. It is up to the cell control system to take into account these variations.

The three fixed supports (with provision of load-cells only) are mounted in order to define the mirror position on the cell (to avoid spurious *tilt* and *piston* terms) and to absorb force residuals after active correction.

Dynamical correction is possible on 3^{rd} order spherical aberration (SPH3), 3^{rd} order astigmatism (AST3), triangular coma (3COM), quadratic astigmatism (4AST) and 5^{th} order coma (COM5). For the reasons discussed above, corrections can be performed in a range limited by the actuator lever system and by the elevation angle; Tab.1 (see also Ref.2) shows the typical allowed ranges for two different elevation angles ($EL = 5.7^0$ and $EL = 23.6^0$).

2.1 Active optics tests made on the primary mirror system

Tests on the primary mirror system have been made in two runs, the first at Ansaldo (Genova) was based on the support cell alone while, during the second run (Zeiss, Oberckoken), the complete system (cell plus mirror) was available on the interferometric tower.

Absolute calibration of load cells has been made using two calibrated sample weights and a simple linear transformation of units.

In fact it was not expected to have, in this way, a good *absolute* calibration; it was more important to have a good estimate of increments or decrements (*relative calibration*) of force because they are directly concerned with the modal correction of the mirror shape. The result of the calibration can be shown in Fig. 1a, 1b where the histograms of the linear regression fits (*off-set* in Kilograms and *gain* in Kilograms/ADU) have been reported. The relative accuracy of the measure is better than 100 grams, while the absolute accuracy depends largely on variations of the *off-set* due to environment changes (temperature, etc.)

In Fig. 2 the histogram of the actuator speeds is reported for a change of force corresponding to the overall allowed dynamic (about 100 *Kilograms*); the average figure of time (about 80 *sec*) can be compared with Tab.1 to have an idea of the actuation speed of the primary system.

Fig. 3.a and 3.b show the phase map of the mirror at the beginning of operations and at the end of the correction procedure. In particular, at the start (Fig. 3.a), the mirror distortion has been dominated, as expected, by astigmatism and spherical aberration (about 1600 nm of spheric and 500 of astigmatism).

After several trials (including also the work to find the correct match between our modal system of coordinates and the one in use at Zeiss) it has been possible to reach a global RMS error, on the wavefront, of about 39 nm. The DEE (*Diffraction Encircled Energy*) computed for the two situations and for the pure diffraction case is reported on Fig. 4.

A calibration of the distortion tables has been independently made for the four active distortion terms applying, one at a time, a cycle of ± 500 nm of distortion (400nm in the quadratic astigmatism case due to system allowed dynamic); in all cases we used a phase angle equal to zero.

Tab.2 shows the results obtained at the end of each cycle; one can show here the resulting errors in terms of:

- required force on actuators against measured force (mean error and RMS);
- required distortion against measured distortion (term by term). This is the true calibration of active modes;

APPLIED DISTORTION		FORCE ERROR		PHASE ERROR		HYSTERESIS	
mode	nm	mean gr	rms gr	nm	angle deg	nm	angle deg
SPH3	500	-33.5	212	-141	—	-37.5	—
AST3	500	-69.7	140.5	-36.9	10.5	2.7	9.5
3COM	500	-27.4	315	67.1	1.1	-1.9	2.18
4AST	400	-21	183.4	-80	3.4	-2.6	0.5

Table 2: Calibration of the primary mirror system.

- resulting cycle hysteresis (term by term).

It is to be noticed that the interpretation of the error for the first two terms (SPH3 and AST3) is somewhat difficult. In fact spherical aberration depends on the distance between mirror and the null-lens system (this distance can change during measurements) and the astigmatism is stimulated by small amount of differential force being it close to the first natural flexure mode of the mirror. This can be easily verified looking at Tab.1; for instance 500 nm of quadratic astigmatism are introduced with 15 peak kg while the same amount of astigmatism is introduced with only 2.5 peak kg.

The hysteresis is computed as the error in magnitude and phase per each term after a complete calibration cycle.

During the correction trials it has been verified the practical possibility to reach a wavefront residual error of about 10 nm RMS for each distortion term. In practice the final accuracy is dominated by astigmatism and 5^{th} order coma residuals.

The 5^{th} order coma residual is concerned with the presence of the three fixed points; we made a simple correction of this unwanted effect introducing a uniform offset force in all astatic actuators. We found, in our case, a rough calibration of $\approx$ 80 nm of 5^{th} order coma per Kg.

Fig. 5.a and 5.b show the 500 nm astigmatism calibration. Fig. 5.b shows the simulated wavefront obtained adding the required astigmatism to the distortion terms already present on the mirror before the force application (this has been done using a mathematical superimposition of Zernicke frames); the result can be compared with the interferogram taken on the mirror as shown in Fig. 5.a.

2.2 Test of the conical constant of the primary mirror

During the test campaign made at Oberkochen we have taken this unique opportunity for a special measurement of the conical constant of the primary mirror. Usually the mirror has been tested through a compensator system of Offner type, due to the very large ($N_\lambda \approx 1312.5$ adopting $\lambda = 500$ nm) spherical aberration introduced by the autocollimation set-up with the (slightly hyperbolical) primary mirror of Galileo.

For a number of reason it was not possible to mount either the secondary mirror or a rail holding a pentaprism over the mirror. This fact lead to the impossibility to perform a test of the whole telescope optics (possible via autocollimation) or the *classical* pentaprism test.

It is to be taken into account, however, that the goal of this special measure was to measure the conical constant of the primary mirror K_1 with an accuracy of the order of one wavelength of spherical aberration in order to rule out problems with the available range of spherical aberration correction via active optics.

Even in this apparently crude measurement, the relative error of the measure is required to be of the order of N_λ^{-1}. This was accomplished using a classical Hartmann screen technique but with the significant modification that the Hartmann screen does not need to be physically placed on the mirror itself (an option ruled out by safety reasons) but it is, instead, projected via a laser beam on the mirror from an apparatus located on the center of curvature of the mirror. The adopted optical layout is sketched, in a simplified form, in Fig.6.

Data were collected on photographic plates. Due to the absence of alluminization of the primary mirror, exposure times lasted up to 15 minutes. Both the small Hartmann screen to be projected on the mirror figure, and the exposed plates, has been digitized using a digitizer machine at the Padova Observatory. In order to improve the accuracy of the digitizing and centroiding of the resulting spots the plates were digitized in two successive steps rotating them of 90°. Moreover the same measurements were performed adopting the set of forces of nearly zero aberrations and

Movement	Range	Required accuracy
x, y (decentering)	$\pm 5mm$	2μm
z (defocussing)	$\pm 10mm$	1μm
α, β (vertex rot.)	± 30"	0.1"

Table 3: Technical specifications for the M2 unit.

introducing $\approx$ 1000nm of spherical aberration in order to check the consistency of the method.

Data has been fitted with a linear and cubic form, and carefully corrected for the (slight) offset introduced by the beam–splitter and for the fact that the test was not performed exactly at the center of curvature (a displacement of $\approx$ 390 mm has been found, leading to $\approx 0.2\lambda$ of spurious spherical aberration). The uncertainty in the determination of the final correction $\Delta K_1 \approx -0.00178$ is much less than the scatter of the measurements, of the order of one wavelength of spherical aberration.

The preliminary (a complete discussion of the reduction procedure and of the error propagation is to be given in a forthcoming paper), corrected for ΔK_1 effects are:

$$K_1^{Sph3=0} = -1.0245 \pm 0.0003 \tag{3}$$

adopting the *best* set of forces, and

$$K_1^{Sph3=1000nm} = -1.0254 \pm 0.0007 \tag{4}$$

introducing, via active optics, $1000nm$ of spherical aberration. Taking into account the nominal value of $K_1 = -1.0238$ and that one wavelength of spherical aberration corresponds to $\delta K_1 \approx 0.0007$ one can conclude that the mirror is close to the expected one, with the uncertainty of the measurements: one wavelength of spherical aberration.

3. THE GALILEO SECONDARY MIRROR SYSTEM

The secondary mirror support design for TNG should fulfill some basic requirements:

1. the mirror positioning should follow the required behaviour in a smooth way (*i.e.* avoiding sleep-stick effects);
2. the mirror positioning should be possible in the overall allowed space;
3. the mirror positioning should be absolute (*i.e.* avoiding the need to reach some reference points at every start-up).

The first and second point have some implications on the way to make exposures on the sky; in fact they should allow the possibility to perform mirror alignment and focus corrections without the need to temporarily stop observations. The last condition should allow the possibility to construct accurate look-up tables of the system behaviour against temperature or other relevant parameters.

All these conditions can be achieved making use of a support structure driven via 6 actuator bars (*exapod* system) shown in Fig.7. Each bar is driven in length by a back-lash free gear system coupled to a motor and absolute encoder, so the relative position between the mirror-holder platform and the fixed platform will be defined by the 6 bar lengths. In fact, in this configuration, each bar will act both as actuator and position measuring system and the secondary will be driven directly commanding the length of each bar.

An advantage derived from the freedom of positioning of the mirror is the possibility to perform rotations both around the *neutral point* and around the *mirror vertex*, allowing separation of coma correction from tilt (see Ref.4).

The main mechanical parameters and expected precisions are given in Tab.3, while in Tab.4 the same values are transformed in bars length parameters.

At the present moment all mechanical parts have been constructed and one bar has been assembled in order to verify the accuracy and hysteresis of movement. The driving electronics and the algorithms making the translation from mirror position to bar lengths have been implemented (see Ref.5).

4. THE GALILEO TERTIARY MIRROR SYSTEM

Movement	Max range	Required accuracy
x, y (decentering)	$\pm 2.83mm$	0.85μm
z (focussing)	$\pm 9.08mm$	0.91μm
α, β (vertex rot.)	$\pm 46.9\mu$m	0.12μm

Table 4: M2 specifications translated to bar length.

Tertiary mirror will allow a fast switch of the light beam on the two Nasmyth focal stations and the quick correction of small tilt errors. It will be equipped with 3 piezo actuators stacks having 40 μm stroke and coupled with three *LVDT* precision position sensors. The tilt possible at the focal plane is of about 8" with a resolution of 0.03" (the tracking performance of the telescope with the autoguider system is specified at 0.05").

The driving electronics for the piezo actuators and *LVDT* sensors has been committed to Physik Instrumente (Germany); the system is also able to make the transformation from orthogonal coordinates to triangular ones (the three actuators are positioned in a triangular way).

A dynamical simulation of the mirror and support structure (see Ref.6) has been made in order to better understand the influences of tilting on the mirror support structure. It has been verified the possibility to act on the system with frequencies lying in the range $10 - 20$ Hz without any appreciable induced error.

5. THE WAVEFRONT ANALYZER AND THE TRACKING SYSTEM

The wavefront analyzer and tracking system for the Galileo telescope will basically follow the NTT design in that two probes will be available in each rotator adapter with the possibility to cover, each one, half of the circular area of 30 arcmin diameter ($336mm$) centered on the derotator axis.

Depending on the field of view covered by the scientific instrument mounted at the derotator focal plane, each probe will cover a half-corona with an area roughly starting from about 100 square arcmin, for an instrument covering a field of 10×10 arcmin, up to about 200 arcmin for an instrument covering 5×5 arcmin.

Nevertheless there are several major differences from the former NTT design; they are concerned with the following requirements:

1. tracking cameras should work also with short integration time (from 10 msec up to few seconds);
2. the Shack-Hartmann (SH) analyzer should be able to provide wavefront parameters (up to the 4^{th} term) *on-line*;
3. the SH analyzer should be able to work, when possible, with short integration time (from 10 msec up to some tens of seconds);

The reason of the first requirement is the need to give a suitable driving signal to the M3 mirror system. This point is critical in that one must take into account the effects (lack of isoplanaticity) due to atmospheric seeing when the guiding probe is far away from the center of the field and when the integration time is short (see Ref.7). Under these circumstances the estimation of the telescope structure tilt can be affected by seeing induced errors. It is clear that a more careful estimation of this problem requires a better knowledge of the Galileo destination site (La Palma, Canary islands) seeing parameters. A way of minimizing the seeing induced error placing several service sensors around the principal CCD sensor mounted on the imaging camera of Galileo is under study.

The main reason of the second requirement is to have the possibility to perform corrections of low-order distortion terms (for instance focus and tilt) during an exposure on the main instrument. Note that the only alternative is to make *look-up table* driven corrections or to stop the exposure.

A further extension to the functions of the SH analyzer is to be able (when a suitable star is available) to make short exposures (although not with fast cycle rate) in order to provide a better seeing characterization at the telescope focal-plane (seeing-monitoring).

In order to fulfill the above requirements it has been decided (see Ref.8) to dedicate one derotator probe only to the tracking function and to place a camera, on the second probe, able to perform three functions:

- a 25×25 sub-pupil SH analyzer;
- a 10×10 sub-pupil SH analyzer;

parameter	10×10	25×25
focal length *fl*	84.8 mm	33.9 mm
lenses diameter *ld*	1.15 mm	460 μm

Table 5: Main design parameters for SH analyzers.

Mode	10×10	25×25
TILT	7.35μm	2.95μm
DEF	14.7μm	5.9μm
4AST	29.4μm	11.8μm

Table 6: SH sensitivity to different distortion orders.

- a star tracker camera.

The switch between modes will be performed inserting three different optics groups in front of the camera. The first option will work with long exposure time (some tens of seconds) and with a limit magnitude of about 16^m, this option will be mainly used for qualification of the optics. The second option will gain about 2^m compared to the first (at the same integration time) and will be used for the *on-line* operation, while the tracking option will be used when the available stars are too faint to allow SH analysis.

Dimensioning the main parameters of the SH camera modes must take into account the need to avoid optics interposed between the SH lenses grid and the camera in order to minimize the light loss and to have optimum spot sampling when the spot size is the smallest (good seeing and short integration time). Under these conditions the remaining free parameter is the detector sensitive area and number of pixels.

Supposing to use a CCD sensor with a sensitive area of 770×576 pixels and a pixel size of 22.5μ (EEV CCD05-20) we obtain the main optical parameters of Tab.5; here we made the assumption to sample the Airy pattern, produced by SH lenses under good and/or short integration time, with 2×2 CCD pixels at $500nm$. The resulting sensitivity of the analyzer (in terms of spot motion on the CCD detector) to different distortion orders (1λ @ $500nm$) is reported in Tab.6.

6. THE CONTROL SYSTEM

The control of the *active optics* system is embedded in a network made of 90 intelligent nodes each one handled by a 16 bits *transputer*.

The *transputer* takes care, in each node, of two main functions:

- the specific application task;
- the handling of communications with neighbours *transputers*, both at *hardware* level (each processor is equipped with four, fast, serial links) and at *software* level (this function is often called *rooting*).

The *rooting* function is implemented on a high priority task which runs, asynchronously, on each node. Care has been taken writing this part of code, in a way to minimize the *rooting* overhead on each node and to minimize to latency when information from various nodes is requested and-or loaded (for instance when all 75 astatic actuators are commanded to a given pattern of values or when all the 75 force map on the primary mirror is requested). With the present software design the latency time is minimal compared with the physical reaction time of commanded devices.

The network topology is fixed, in that all links are hardwired, and it has been designed having in mind the need to minimize the number of intermediate nodes needed to reach a given node. When the physical distance between nodes is longer than one meter, the link connection has been made interposing commercial fiber-optics link adapters.

Fig.8 reports the distribution of main parts forming the control net. One can identify the three main blocks concerned with the three telescope mirrors and the connection to the telescope control network (basically an *ethernet* system) through a VME crate.

The block *M1-CONTROL* holds a mesh of 75 nodes each one equipped with a motor-controller driver and a load-cell readout circuit. A node, in this block, can:

- set the corresponding actuator to a given force;
- handle a circular queue with last 50 load-cell measurements;
- close a *position* loop between motor driver and load-cell (*i.e.* to hold the required force in a dynamical way);
- correct forces when the EL angle is changing.

The blocks *M2-CONTROL* and *M3-CONTROL* are similar in principle, with several differences concerned with the kind of actuators and sensors handled. *M2-CONTROL* is based on a *pipe-line* of 6 nodes while *M3-CONTROL* is handled by a single node.

5. CONCLUSIONS

The active optics system of the Galileo telescope is in an advanced stage of qualification. It has been demonstrated that the primary mirror system can reach the level of optical quality and the possibility of active intervent as required from the specifications. The control system dedicated to the active optics as also been tested; the concept of a distributed network of *transputer* to handle the system, from wavefront analyzer cameras up to mirror actuators, fulfills all specification requirements.

6. ACKNOWLEDGEMENTS

Thanks are due to all the TNG project team. Special thanks are given to the Director Prof. C. Barbieri and to the overall technical staff who made possible the completion of tests made in Ansaldo (Genova) and Zeiss (Oberckoken), in particular the personnel of the Padova and Catania Astronomical Observatories.

5. REFERENCES

1. Bortoletto, Bonoli, Fantinel, Ragazzoni, Giudici, Vanini, Gallieni, Tommelleri, ESO proc. **42**, 323, (1992)
2. Wilson et al., IAU colloquium **79**, 23, (1984)
3. Schwesinger, J. of Mod. Opt.,**35**, 1117, (1988)
4. Ragazzoni, Bortoletto, SPIE *proc.* **1542**, 236, (1991)
5. Bortoletto, Ragazzoni, "Specifiche software per l'unitá M2", TNG technical report, september 1991
6. Gatti,"Verifiche statiche e dinamiche strutture e sopporti M2 ed M3", ADS, september 1991
7. Wilson, Noethe, SPIE *proc.* **1114**, , (1989)
8. D'Alessandro, Ragazzoni, Bhatia, Bonaccini, Bortoletto, Conconi, "Il rotator-adapter per Galileo", november 1993

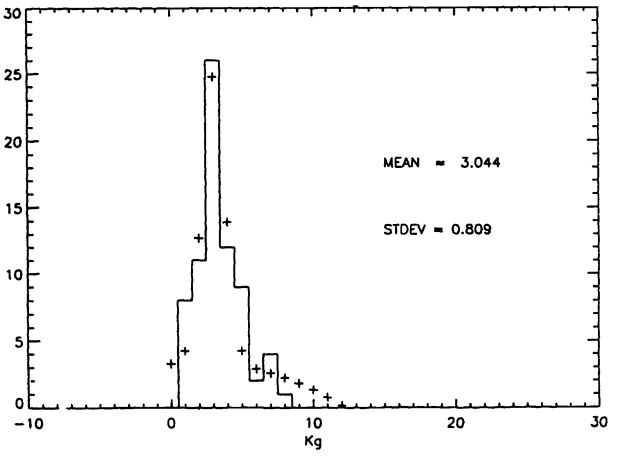

Figure 1a M1 supports off-set calibration histogram.

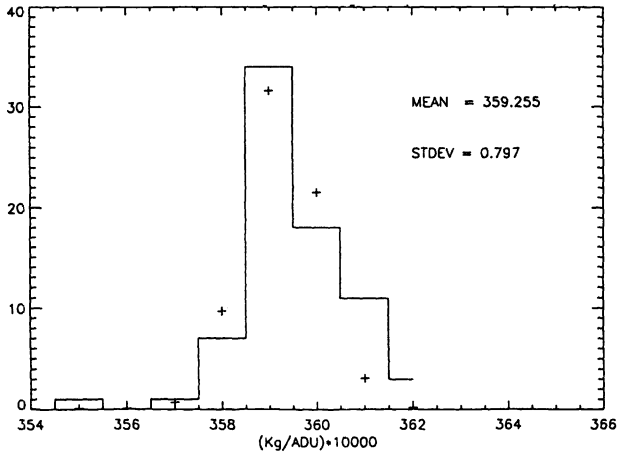

Figure 1b M1 supports gain calibration histogram.

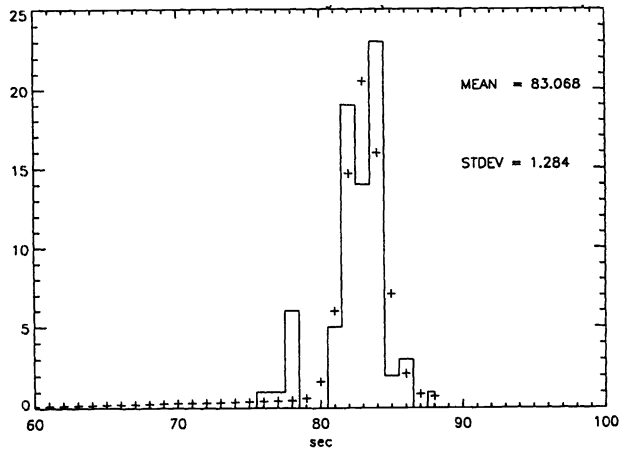

Figure 2 M1 supports time histogram for full dynamic range ($\pm 25 Kg$).

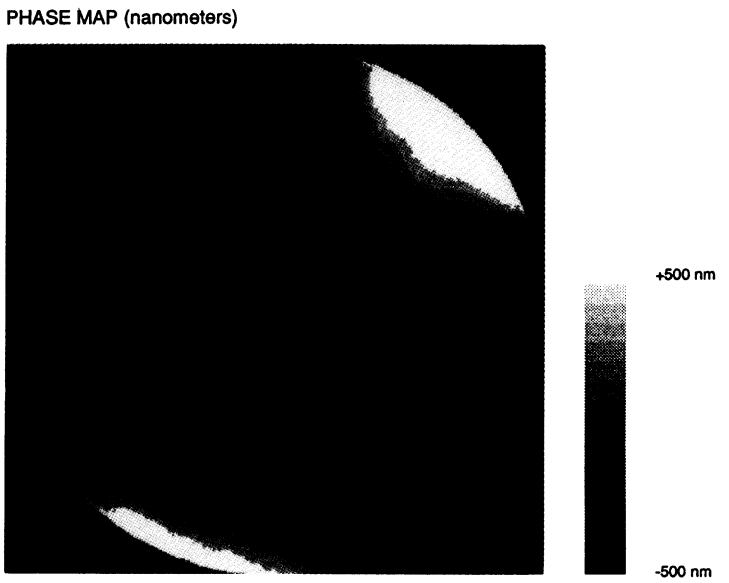

Figure 3a.Interferogram of M1 before active corrections. Total RMS error is 207 *nm.*

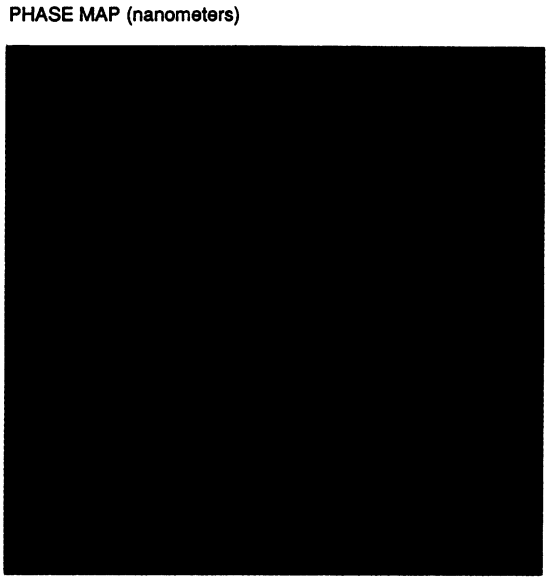

Figure 3b. Interferogram of M1 after active corrections. Total RMS error is 39.7 *nm.*

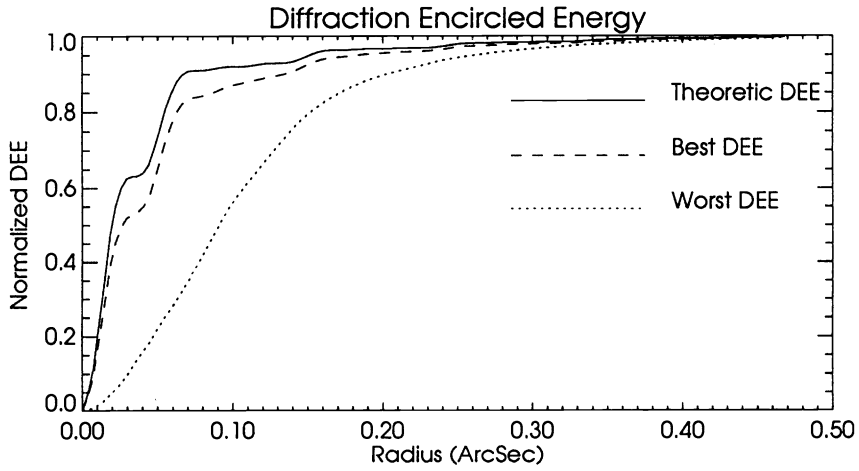

Figure 4. DEE computed for situations shown in Fig. 3a and 3b.

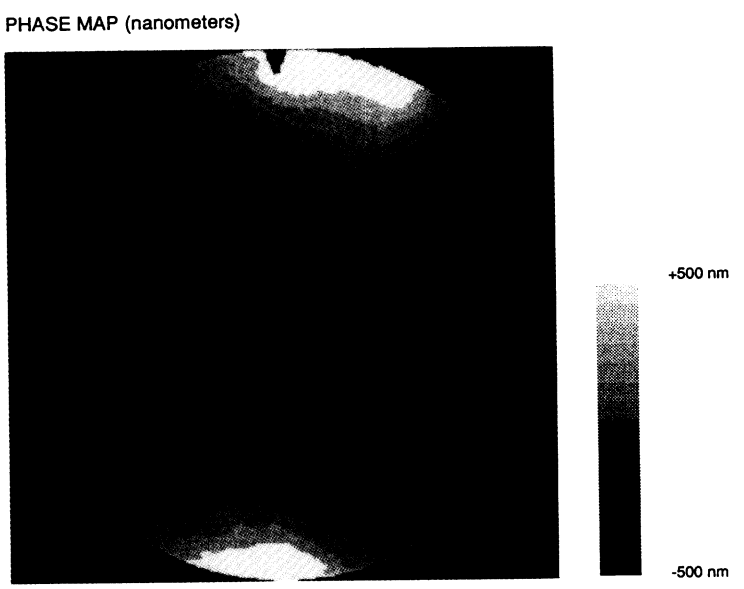

Figure 5a. M2 mirror interferogram after application of 500 nm of astigmatism.

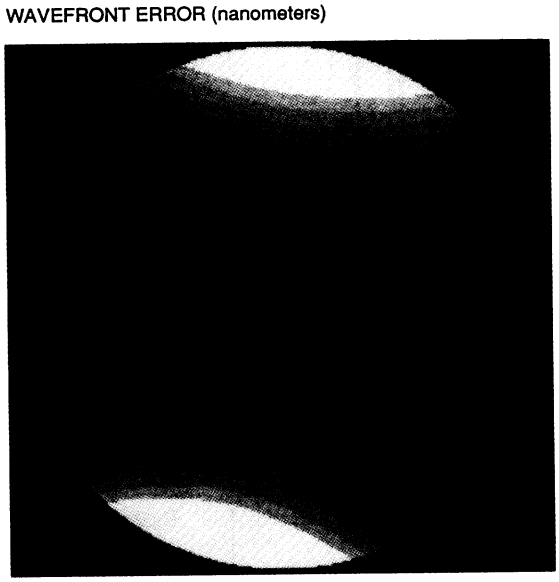

Figure 5b. Simulated wavefront for the situation in Fig. 5a.

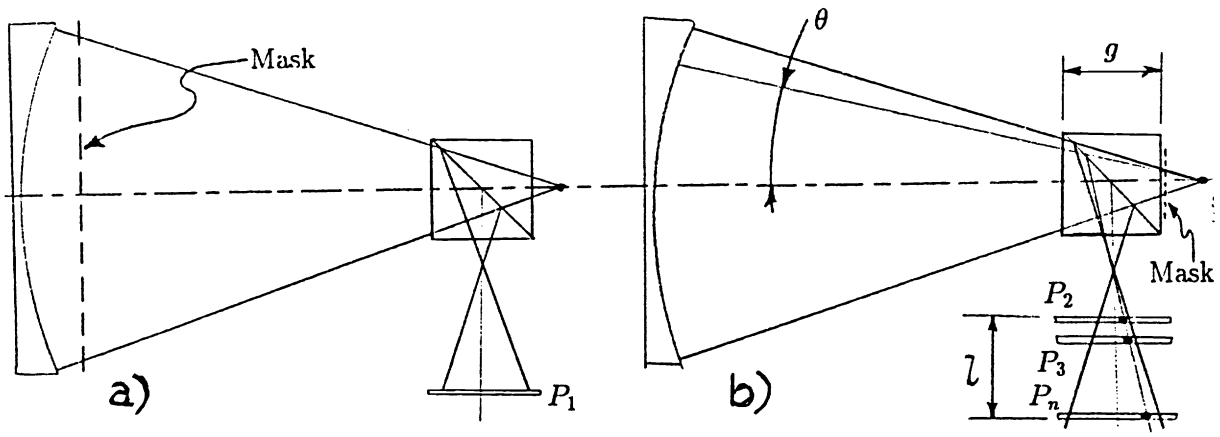

Figure 6a: Scheme of the classical Hartmann test; Figure 6b: The modified scheme. The mask is projected onto the mirror and the returning spots are collected by plates located in various positions $P_2 \ldots P_n$ spanning an l range. This is necessary because projecting the mask on the mirror the absolute calibration of the position of spots on the mirror is lost. This information can be gained through the knowledge of the angle θ via fitting straight lines on the spots collected by the different plates.

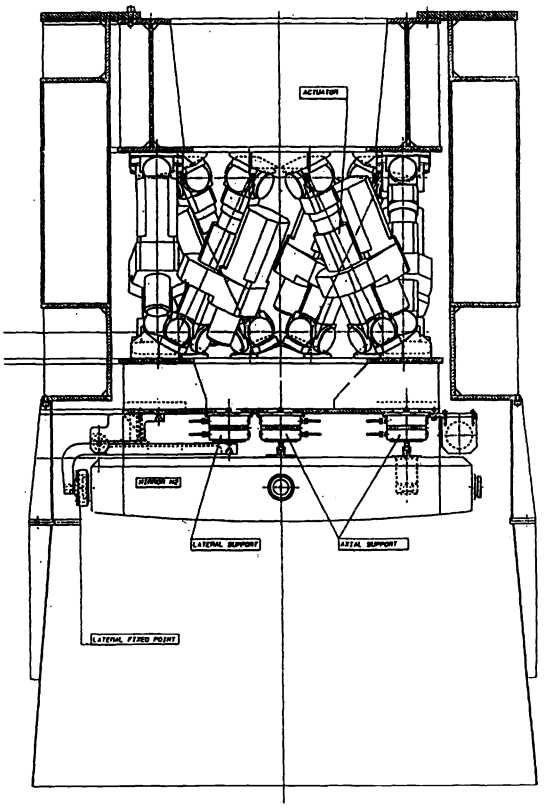

Figure 7. The M2 mirror support and positioning system.

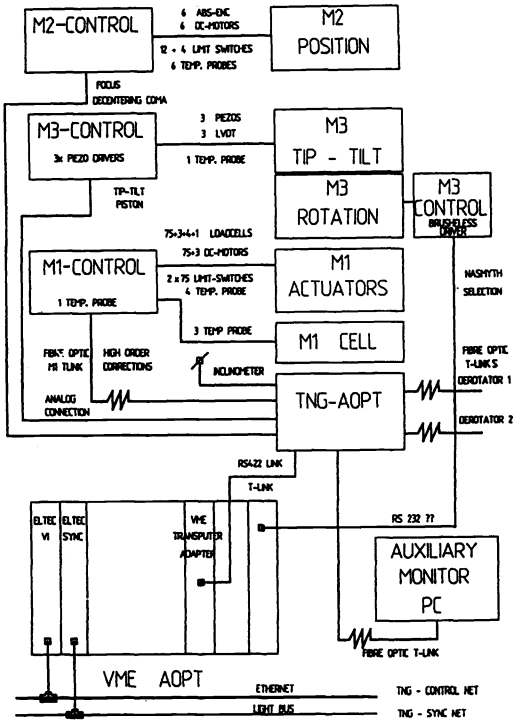

Figure 8. The active optics control system and communication network.